

Free-Flyer Acquisition of Spinning Objects with Gecko-Inspired Adhesives

Matthew A. Estrada,* Benjamin Hockman,* Andrew Bylard,* Elliot W. Hawkes, Mark R. Cutkosky, and Marco Pavone

Abstract— We explore the use of grippers with gecko-inspired adhesives for spacecraft docking and acquisition of tumbling objects in microgravity. Towards the goal of autonomous object manipulation in space, adhesive grippers mounted on planar free-floating platforms are shown to be tolerant of a range of incoming linear and angular velocities. Through modeling, simulations, and experiments, we characterize the dynamic “grasping envelope” for successful acquisition and derive insights to inform future gripper designs and grasping strategies for motion planning.

I. INTRODUCTION

Robotic manipulators capable of reliably attaching and detaching from target objects are critical to many ongoing and emerging space-based applications (e.g., docking maneuvers, orbital debris removal, and on-orbit servicing). Recently, there has been a particular interest in small assistive free-flyers that could grasp and manipulate payloads inside and outside space vehicles [1]–[3]. Ideally, their grippers would also enable them to dock onto the external hulls of spacecraft and debris for monitoring, repair, or object redirection.

Traditional approaches to grasping use hands or grippers that either compress opposing faces of the target to generate friction (as in the International Space Station’s Canadarm), or grapple around features to lock the object in place (as in the Orbital Express Capture System). An extensive literature addresses grasp planning with internal forces and friction [4]. However, conventional grippers often require “cooperative” targets with low speeds relative to the manipulator. Even when catching fast-moving objects (e.g., [5]), or when grasping objects from a flying or floating platform [6]–[10], the context generally assumes an uncluttered workspace so that the hand or gripper can wrap around the object or grappling fixture to grasp it with internal forces.

Alternatives include astrictive grippers [11] that hold an object using suction or electrostatic attraction, etc. However, suction will clearly not work in a vacuum (e.g. outside a space vehicle) and electrostatics may pose a concern when handling electronics. In addition, most astrictive grippers require the continual provision of power.

Instead, practical solutions can be found in “contigutive” grippers [11], which rely on contact and surface adhesion.

M.A. Estrada, E.W. Hawkes, and M.R. Cutkosky are with the Mechanical Engineering Dept., Stanford University. B. Hockman, A. Bylard, and M. Pavone are with the Aeronautics and Astronautics Dept., Stanford University, Stanford, CA 94305.

Emails: {estrada1, b.hockman, bylard, ewhawkes, cutkosky, pavone} @stanford.edu

*These authors contributed equally to this work.



Fig. 1. Grasping with flexible dry adhesives stands to unlock capabilities for assistive free-flyers, such as the SPHERES robot shown here. Grasping surfaces, rather than specific features, offers new strategies for manipulation.

Examples of contigutive grasping range from adhesives used for micro-assembly [12], [13] to grasping large items, such as solar panels, in space using gecko-inspired dry adhesives. These adhesives exploit *controllable adhesion*, which allows rapid attachment and detachment with minimal interaction force, critical for zero or micro-gravity operations [14]. The fibers can be deposited on flexible films, allowing grippers to conform to smooth or moderately textured flat or curved surfaces [15]. The materials are passive, and space-qualified versions have undergone environmental testing aimed at space applications [14], [16], [17].

Dry adhesive grippers show unique promise for docking with or capturing “uncooperative” targets having significant relative translational and rotational velocity. To the authors’ knowledge, this work is the first example of capturing and stabilizing translating and spinning objects with gecko-inspired adhesion. This work with planar free-flyers is a first step toward object acquisition and manipulation in space.

The contributions of this paper are: (i) the design of a new gripper and wrist mechanism that utilizes controllable dry adhesives and has appropriate compliance to capture and subsequently stabilize a moving, spinning object; (ii) models of the dynamic gripper/object interaction that provide insights for design and control and (iii) the results of experiments with planar free-flyers acquiring objects, which confirm predictions from the dynamic models and provide additional insights for future work. An interesting result is that the acquisition region, which determines how far the

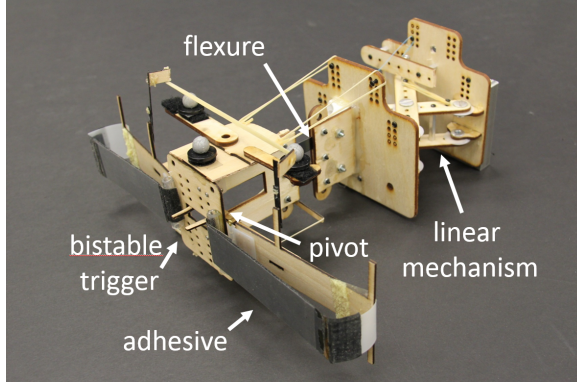


Fig. 2. Adhesive gripper and compliant wrist for acquiring and stabilizing moving, spinning objects.

gripper can be offset from the line of approach of the object, depends strongly on the relative angular velocity. Taking this into consideration allows for solutions in which the gripper gently touches a spinning object and effectively rolls or wraps into a stable grasp.

II. GRIPPER DESIGN

A. Curved Surface Gripping

The presented gripper makes use of recent developments in the grasping of convex surfaces using gecko-inspired adhesives deposited on a thin film. When the adhesive contacts a surface and shear stress is applied in the film's preferred direction, the fibers lay against the surface and adhere to it [15].

The gripper presented here is composed of two opposing flexible adhesive films, each held taut by a hinged, bistable arm mechanism mounted on a frame, as depicted in Fig. 3A. When a surface pushes against the triggers, the arms collapse, engaging the adhesive films (Fig. 3B). The films conform to convex surfaces and adhere, after which significant normal and shear forces and moments can be applied (Fig. 3C). The span of the gripper is 26 cm, with each arm holding a 3×9 cm adhesive film for a total adhesive area of 54 cm^2 .

B. Compliant Gripper Wrist

Linear and rotational compliance in the wrist mechanism enables the gripper to passively align to target objects and dissipate kinetic energy.

For ease of adjustment, the wrist mechanism is split into three separable compliance elements. The gripper is mounted on a hinge providing rotational compliance. The hinge is attached to a flexure which adds transverse compliance, followed by a linear mechanism that provides compliance in the normal direction (Fig. 3D).

Since this work focuses on initial capture and absorption of kinetic energy to maintain grip, only springs were considered in the design. In future work, additional damping will suppress oscillations after object acquisition.

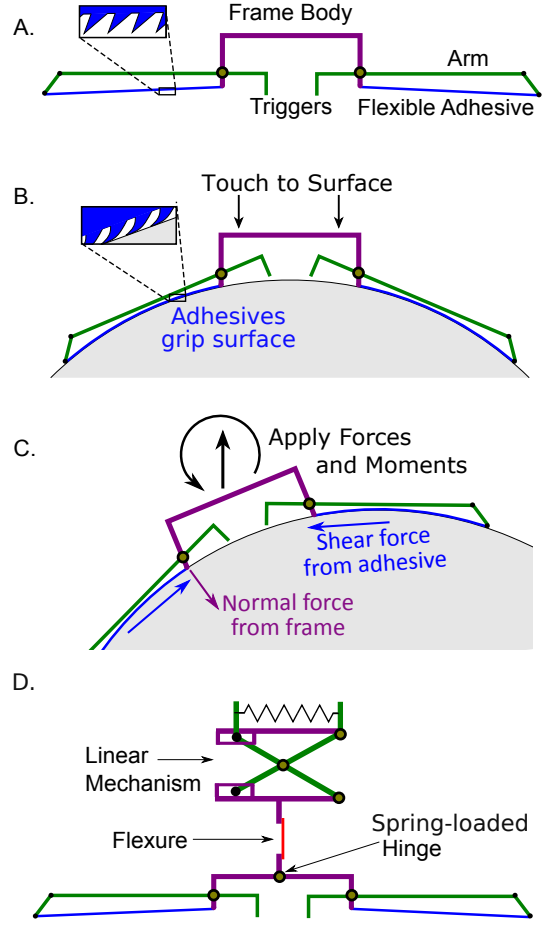


Fig. 3. (A) Diagram of the flexible adhesive gripper. (B) When touched gently to a surface, the triggers collapse the bistable arms, wrapping the adhesive around the object. (C) Once the film is engaged with the surface, forces and moments can be applied. (D) Wrist mechanism with decoupled compliance in normal, transverse, and rotational directions.

III. DYNAMIC MODELING

This section proposes two dynamic models that provide complimentary insights into the process of gripper/object interactions, and how to characterize and leverage the robust properties of curved surface grippers.

A. Impact as a Perfectly Inelastic Collision

As a starting point, a very simple planar inelastic collision model provides some useful first-order insights into how energy is dissipated upon gripper engagement. For scenarios where an object impacts at the center of the gripper, the gripper arms immediately collapse and engage the object. Such engagements can be modeled to a good approximation as purely inelastic collision at the center-point of the gripper. That is, once the gripper and object collide, they both rotate about the pivot point as a single rigid body (see Fig. 4).

This inelastic assumption enables a closed-form solution and provides an intuitive sense for how much energy will be dissipated during initial impact. For simplicity, we ignore non-rotational compliance in the gripper and assume its mass is negligible compared to the target object's mass. Indeed, the translational compliance in our gripper is much stiffer than

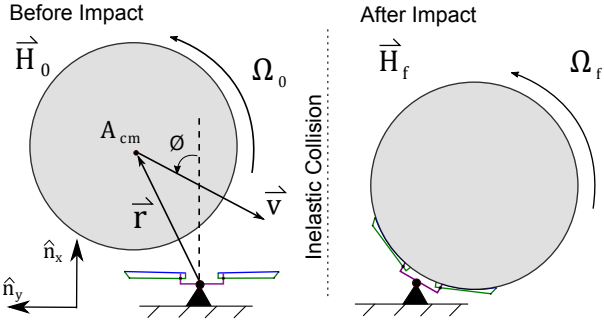


Fig. 4. An estimate of energy dissipated during impact can be calculated from the conservation of angular momentum about the gripper's pivot point during a perfectly inelastic impact.

the rotational compliance, and the object has 30 times more mass than the gripper. The results of this model extend to other situations in which two free-floating objects approach each other with a high kinetic energy but zero net angular momentum.

Assuming the pivoting hinge at the center of the gripper exerts negligible moments during impact, [18] expresses conservation of angular momentum about the pivot point:

$$\vec{H}_0^{N_{pivot}} = \vec{H}_f^{N_{pivot}}$$

$$\vec{r} \times m\vec{v} + I_{zz}^{A_{cm}}\Omega_0\vec{n}_z = (I_{zz}^{A_{cm}} + m\|\vec{r}\|^2) \cdot \Omega_f\vec{n}_z \quad (1)$$

Where variables include the object's moment of inertia taken about its center of mass ($I_{zz}^{A_{cm}}$), the angular velocity of the object before (Ω_0) and after (Ω_f) impact, and the object's incoming velocity (\vec{v}). Rearranging terms, we find the angular velocity of the object post-collision as it rotates about the gripper pivot joint:

$$\Omega_f = \frac{(\vec{r} \times m\vec{v}) \cdot \vec{n}_z + I_{zz}^{A_{cm}}\Omega_0}{I_{zz}^{A_{cm}} + m\|\vec{r}\|^2} \quad (2)$$

We can now derive the kinetic energy lost in the collision, expressing the cross product in terms of the incoming angle of attack, ϕ :

$$K_0 - K_f = \frac{1}{2}I_{zz}^{A_{cm}}\Omega_0^2 + \frac{1}{2}m\|\vec{v}\|^2 - \frac{1}{2} \frac{(m\|\vec{r}\|\|\vec{v}\|\sin\phi + I_{zz}^{A_{cm}}\Omega_0)^2}{I_{zz}^{A_{cm}} + m\|\vec{r}\|^2} \quad (3)$$

This result gives practical considerations for engaging rotating objects, through either gentle grasps or sudden decelerations. Eqn. (3) suggests that for objects with or without spin, energy dissipation on collision can be minimized by reducing the relative linear velocity between the contacting surfaces. In particular, given an object with some angular velocity, initial energy dissipation can be reduced by increasing angle

of attack or altering the free-flyer's transverse velocity with respect to the object.

Conversely, to dissipate the maximum amount of energy upon impact, one should aim for zero net angular momentum about the pivot point (i.e. when the linear and angular components the last term of Eqn. (3) cancel out). An experimental comparison between these two situations is seen in Section IV-D.

B. Numerical Model

Simplified and decoupled models of adhesives and compliant mechanisms help to provide first-order analytic insights into gripper behavior. However, a more comprehensive model is required to understand the gripper response during collisions where the object hits significantly off-center, when the system dynamics are highly coupled. Through numerical simulations, such a model can help to understand failure modes, characterize the grasping envelope, and provide design insights for the gripper.

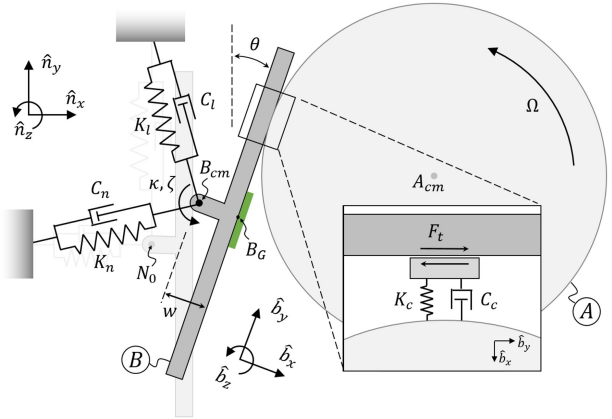


Fig. 5. Dynamic model of gripper. The generalized compliant fixture (6 springs/dampers) can capture the response of a variety of wrist mechanisms.

Consider the 2D model shown in Fig. 5, which consists of two (massive) rigid bodies: the floating object (A) and the gripper (B). While there are inherent limitations with a planar model, as a first pass, it is sufficient for comparison with our 2D experimental setup (see Fig. 6), and indeed can capture the full 3D case when the object's spin axis is aligned with the gripper's hinge axis.

The gripper, also floating in the plane, is mounted to the free flying spacecraft through a series of springs and dampers (linear and torsional), which can be tuned to capture the compliance in the gripper's wrist¹. Although the gripper actually consists of two arms hinged to a common frame body, prior to grasping, these three rigid bodies are initially *locked together* by the bistable mechanism and can be treated as a single rigid body. The interaction between the gripper and object is modeled as a deformable contact by normal spring/damper forces. Although detailed models of grasping with directional adhesion are available [15], [19],

¹Here, for simplicity, we treat the spacecraft as an inertial frame, which is a good approximation for a large spacecraft grasping a smaller object.

the gripper/object contact in the current application produces a positive normal pressure immediately on contact, so that one can approximate the adhesive limit with anisotropic friction:

$$|F_t| \leq \begin{cases} F_{t,min} + \alpha F_n, & \text{in adhesive direction} \\ \mu F_n, & \text{against adhesive direction} \end{cases} \quad (4)$$

This model is shown to be in agreement with experimental data in Section IV.

With the forces from the elastic fixture and contact model, the equations of motion for each body simply follow from Newton's second law, yielding a 12 state system (3 position and 3 velocity for each body).

Because this formulation treats the gripper as a single rigid body and cannot "lock on" to the object, a "graspable state" must be defined in order to compare simulations with the binary success/failure results from experiments. The grasping criteria are defined as:

- 1) Object contacts gripper within δ_x offset from B_G , AND
- 2) $|\Omega| < \Omega_{max}$

The first criterion is illustrated by the green shaded region in Fig. 5. The second criterion captures the gripper's inability to grasp (even well positioned) fast spinning objects. As discussed in Section IV, these criteria match experimental observations.

IV. FREE-FLYER EXPERIMENTS

Grasping experiments were conducted on the Stanford free-flyer testbed—a 2D microgravity analog consisting of a 3x4 m 20 ton granite table with a precisely calibrated flat and level surface, on which robotic platforms can drift on air bearings with near-zero friction (see Fig. 6).

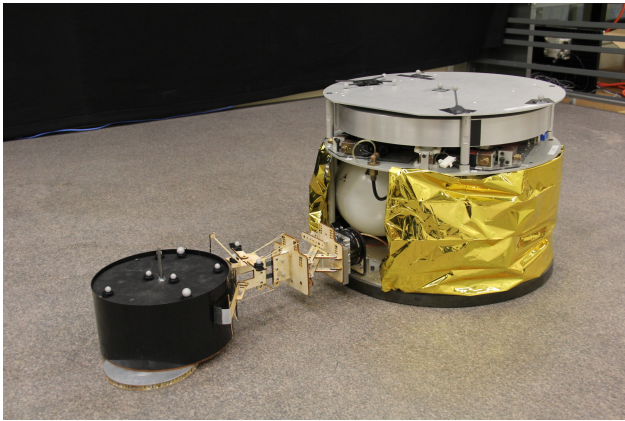


Fig. 6. The free-flyer testbed uses air bearings to hover on a granite table to simulate a frictionless zero gravity environment. Shown here is a small "floating" cylindrical object being grasped by a larger free-flyer with a flexible dry adhesive gripper.

A smooth cylinder was mounted on a floating platform to act as a uniform, curved object to be grasped. The 23 cm

diameter target object had a mass of 1.55 kg and inertia of 0.013 kg·m². The motions of both the gripper and object were tracked and recorded to sub-millimeter precision using an OptiTrack motion capture system running at 120 Hz.

The goal of these experiments was to characterize the tolerance of the curved surface gripper to relative momentum and misalignment. Specifically, the initial contact state can be uniquely described by four parameters: relative velocity, both linear (v) and angular (Ω), angle of attack (ϕ), and lateral offset (d) from the center of the gripper (summarized in Fig. 7). To have more control over these parameters for repeatable experiments, the gripper was *fixed* to the table, and the object was guided into it. While this is comparable to the case of a massive free-flyer grasping a small object, it also reflects many other situations with similar relative momentum.

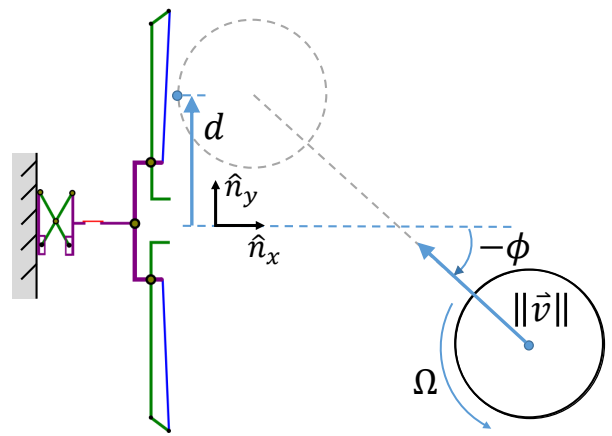


Fig. 7. Parameters defining the object's incoming state: magnitude of linear (v) and angular velocity (Ω), offset of the initial contact point from gripper center (d) measured along \hat{n}_y , and angle of attack (ϕ).

A. Dynamic Grasping of Non-Spinning Objects

As a first step, we consider the problem of capturing objects that are translating but not rotating. As seen in Fig. 8, the presented gripper is capable of capturing objects with speeds of up to 1 m/s and approach angles of up to 70°.

Predictable failures were observed at very low speeds, as the gripper requires sufficient linear momentum *normal to the surface* (around 0.15 kg m/s) to compress the triggers and collapse the bistable mechanism, as shown by region A in Fig. 8). Note that this lower bound can be tuned by adjusting the stiffness of the bistable mechanism or removed entirely by using an actuator for grasping.

In contrast, fast approaches from sharp angles confront the gripper with high angular momentum (taken about the gripper's wrist) and require larger moments to be arrested, often causing disengagement. This poses a (soft) limit on the angular momentum of the system that can be tolerated after impact, as denoted by region B in Fig. 8.

Since the gripper opens flat in its default state, there is no inherent limitation in its ability to grasp incoming objects

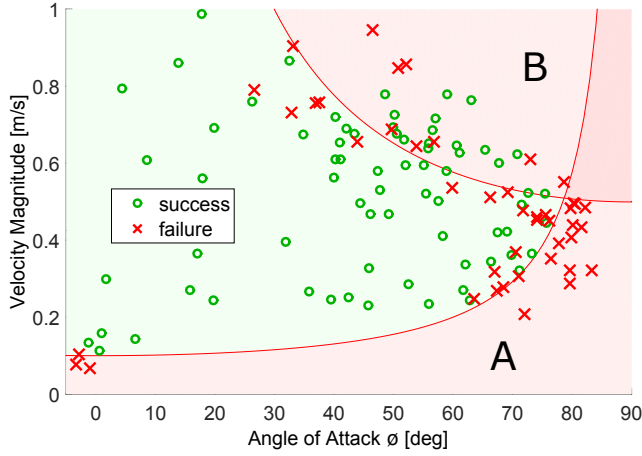


Fig. 8. Probing the boundary of tolerable grasping conditions with a focus on relative velocity. Angular velocity is kept very close to zero. Two limits help to separate success and failure: (A) a minimum linear momentum normal to the gripper required to collapse the bistable mechanism and (B) a maximum angular momentum that can be arrested.

at large angles of attack. However, as expected, contacting the gripper near its center requires more precise “aiming” at steep angles of attack, where even slight deviations in heading can produce drastic transverse offsets.

As discussed in the perching literature, these baseline results also inform how grasping robustness can be affected not only by the gripper itself, but especially by the compliance of the supporting structure. In general, more compliance and higher potential for energy absorption can help to reduce peak forces and prevent disengagement.

B. Grasping of Spinning Objects

Oftentimes in space, free-floating objects we may want to grasp will be tumbling with some relative angular velocity—a difficult situation for traditional feature grasping. Surface grasping, however, has the potential to be highly tolerant to relative spin and could therefore be a uniquely capable technology for such applications. Towards this goal, a series of grasping experiments were conducted on rotating objects.

One of the most important decisions a spacecraft must make in order to successfully engage a spinning object is how to position its gripper. As a first set of experiments, this key parameter, offset (d), was varied along with angular velocity (Ω), using zero angle of attack (mean $\mu_\phi = 1.5^\circ$ and standard deviation $\sigma_\phi = 2.6^\circ$) and a nominally constant velocity ($\mu_v = 0.27 \text{ m/s}$, $\sigma_v = 0.06 \text{ m/s}$).

The grasping envelope for this data is plotted in Fig. 9. As a means of comparison and validation of our model proposed in Section III-B, numerical simulations were also run over a swept range of initial conditions (1000 in total). The green shaded region in Fig. 9 encloses the initial conditions for which the model predicts a successful grasp, based on the success criteria outlined in Section III-B. The simulated success region correlated with our experimental trials.

Intuitively, it makes sense that the grasping envelope is a

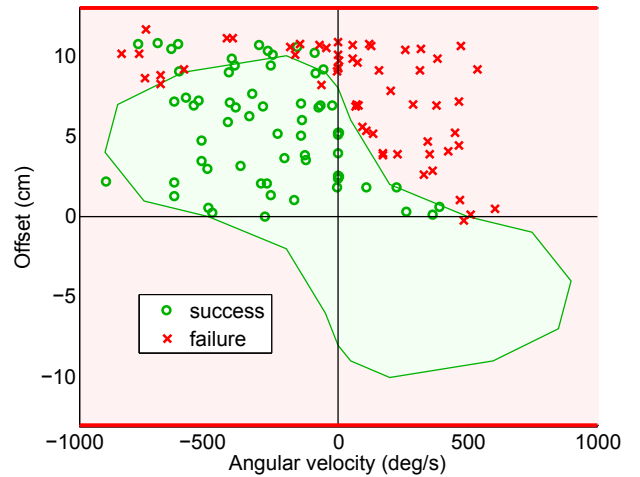


Fig. 9. Grasping envelope for an object with spin (Ω) and offset (d). The green shaded region encloses the predicted success based on the numerical model. Due to the inherent symmetry in the gripper and cylindrical object, data was only collected for the half-plane.

relatively smooth region centered at the origin; high offsets glance off to the side and high angular velocities are beyond the energy dissipation limitations of the gripper. Particularly interesting, however, is the shape of the envelope and its apparent “quadrant bias”. In other words, while some level of spin is tolerable on either side of the gripper, grasping is much more robust when the object spins *into* the center of the gripper. This can inform motion planning algorithms on autonomous free-flyers that, given a target object with certain spin characteristics, intentionally engaging with a bit of misalignment can be beneficial.

C. Grasping at Oblique Orientations

Towards the most general grasping case with nonzero velocity, angular velocity, offset, and angle of attack, a similar set of experiments was performed as in Section IV-B, this time at a non-trivial angle of attack ($\mu_\phi = 44^\circ$, and $\sigma_\phi = 2.6^\circ$) and with a similar speed ($\mu_v = 0.34 \text{ m/s}$, $\sigma_v = 0.05 \text{ m/s}$).

The results shown in Fig. 10 exhibit a similar grasping envelope as in Fig. 9. Again, the green shaded region generated from simulations with swept initial conditions is a reasonable partition between successful and unsuccessful trials. Interestingly, it has a much different (asymmetric) shape and is heavily biased towards quadrant II. So in this case, not only is it beneficial to spin into the center of the gripper, but there is also a strong preference for striking the *near* side of the gripper. Indeed, this effect can also be explained by the analytical impact model proposed in Section III-A: quadrant II corresponds to the case requiring the least energy dissipation.

Another way of looking at these grasping envelopes is as 2-D *slices* within a larger 4-D manifold. Because gripper-equipped free-flyers have little control over the object’s spin and relative velocity (at least in the vicinity of engagement),

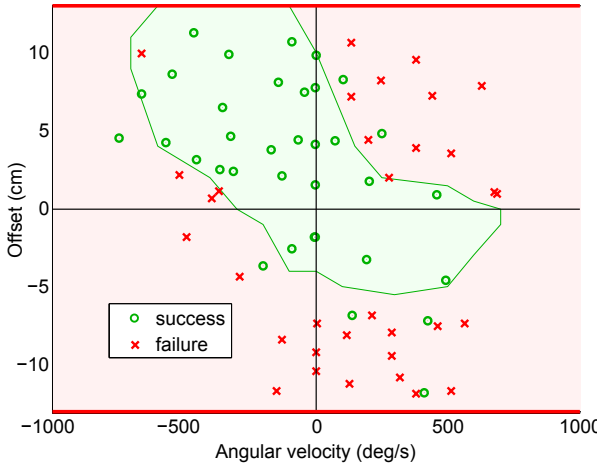


Fig. 10. Grasping envelope for spinning objects at a 45° angle of attack. The green shaded region encloses the predicted success based on the numerical model.

these 2-D slices can help them decide how to control their relative alignment (d) and orientation (ϕ) to increase their chances of a successful grasp. For example, a non-spinning object has the greatest offset tolerance with a head-on engagement (i.e. $\phi = 0$ in Fig. 9), whereas a slowly spinning object may be more robustly captured at an oblique angle of attack (i.e. $\phi < 0$ in Fig. 10).

D. Angular Momentum and Energy Dissipation

Net angular momentum was observed to have a large effect on the gripper dynamics after engagement. Consider two similar cases depicted in Fig. 11. In each case, the objects approach at a 45° angle of attack, have similar linear velocities, and have the same offset and angular velocity magnitude. However, the direction of the spin is reversed, resulting in a large disparity in the incoming angular momentum of each object, calculated about the gripper's hinge joint.

Notice the very different behaviors in Fig. 11 with the “despin” maneuver dissipating much more energy than the “rolling” engagement. Making the gross assumption that angular momentum is held constant during an inelastic impact, as detailed in Section III-A, the calculated kinetic energy before and after impact is superimposed on the plot.

With appreciable compliance in the gripper’s wrist, the assumption of a rigid impact deviates from reality. The “despin” maneuver recovers a portion of the model’s dissipated energy from the energy stored in the flexure mounted behind the pivoting joint. The rolling case likely experiences extra energy dissipation through slippage at the adhesive’s surface before engaging and pivoting. Even with these second-order effects considered, a perfectly inelastic collision provides intuitive insight for attachment maneuvers.

V. CONCLUSIONS AND FUTURE WORK

Our curved surface gripper has been shown to successfully grasp a rotating object with a wide range of linear and rotational velocities. Models show that energy dissipation in

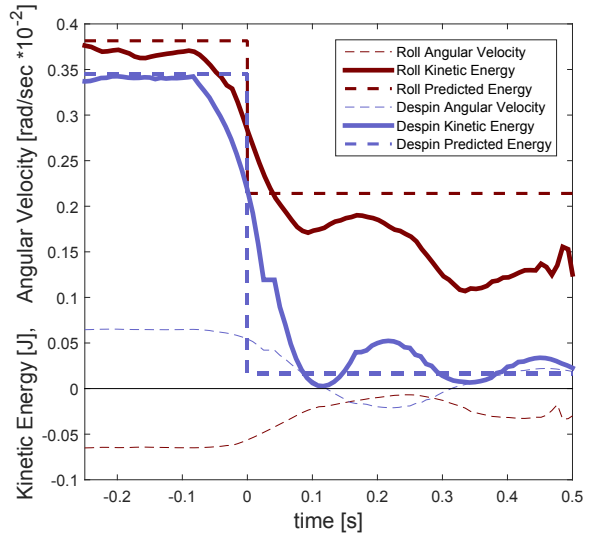


Fig. 11. Demonstration of maximum energy dissipation on collision in “despin” scenarios, characterized by net zero angular momentum, vs. the case where spin is in the opposite direction, where a “rolling” effect occurs.

the first moments of impact is highly dependent upon the net angular velocity of the system. Calculating energy dissipated during collision sheds light on whether the gripper can remain attached as an object comes to rest within its grasp. Additionally, an object’s interaction with the adhesive before attachment can either push it into a successful engagement or vice versa.

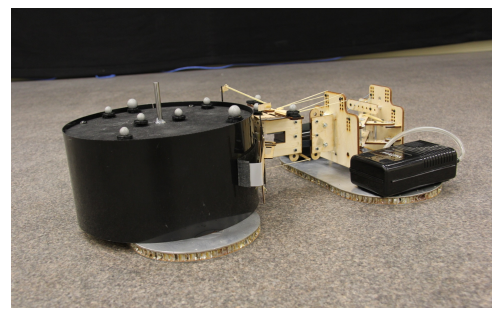


Fig. 12. Gripper mounted on a lightweight floating platform for small-target grasping experiments.

A gripper capable of attaching under a variety of incoming conditions opens the possibility of manipulation utilizing a free-flyer’s momentum. Tolerance to parameters such as offset in the gripper’s attachment point, an oblique angle of attack, and relative angular velocity all provide degrees of freedom to shape the angular momentum of an incoming platform. Considering the net momentum of the free-flyer and grasped object will be a sum of the parts, a robotic

system could use its incoming conditions to augment the final momentum of the joined bodies.

An area of interest for future work involves grasping of a target similarly sized to the free-flyer (Fig. 12). Initial modeling and experiments suggest that we will find very similar results to the case considered in this paper, where the target is anchored.

Moving to full 3-D grasping and docking is another future direction. It is possible the gripper may require a second, orthogonal set of adhesives to aid in managing arbitrary spins.

ACKNOWLEDGMENT

This work was partially supported by NASA under the Space Technology Research Grants Program, Grant NNX12AQ43G and by NSF IIS-1161679 and ARL MAST MCE 14-4. M. Estrada, B. Hockman, were supported by the NSF Graduate Research Fellowship. A. Bylard was supported by the NASA Space Technology Research Fellowship, Grant NNX15AP67H. We thank Hao Jiang for his extensive advice on gripper design and implementation.

REFERENCES

- [1] S. A. A. Moosavian and E. Papadopoulos, “Free-flying robots in space: an overview of dynamics modeling, planning and control,” *Robotica*, vol. 25, pp. 537–547, 9 2007.
- [2] M. Bualat, J. Barlow, T. Fong, C. Provencher, and T. Smith, “Astrobee: Developing a free-flying robot for the International Space Station,” in *Proc. AIAA Space Forum*. IEEE, 2015.
- [3] C. Menon, M. Murphy, F. Angrilli, and M. Sitti, “Waalbots for space applications,” in *55th IAC Conference, Vancouver, Canada*, 2004.
- [4] D. Prattichizzo and J. Trinkle, “Grasping,” in *Springer Handbook of Robotics*, B. Siciliano and O. Khatib, Eds. Springer Berlin Heidelberg, 2008, pp. 671–700.
- [5] A. Namiki, Y. Imai, M. Ishikawa, and M. Kaneko, “Development of a high-speed multifingered hand system and its application to catching,” in *Intelligent Robots and Systems, 2003. (IROS 2003). Proceedings. 2003 IEEE/RSJ International Conference on*, vol. 3, Oct 2003, pp. 2666–2671 vol.3.
- [6] D. Mellinger, Q. Lindsey, M. Shomin, and V. Kumar, “Design, modeling, estimation and control for aerial grasping and manipulation,” in *Intelligent Robots and Systems (IROS), 2011 IEEE/RSJ International Conference on*, Sept 2011, pp. 2668–2673.
- [7] P. E. Pounds, D. R. Bersak, and A. M. Dollar, “The yale aerial manipulator: grasping in flight,” in *Robotics and Automation (ICRA), 2011 IEEE International Conference on*. IEEE, 2011, pp. 2974–2975.
- [8] D. Mellinger, M. Shomin, N. Michael, and V. Kumar, “Cooperative grasping and transport using multiple quadrotors,” in *Distributed autonomous robotic systems*. Springer, 2013, pp. 545–558.
- [9] D. Hirano, K. Nagaoka, and K. Yoshida, “Design of underactuated hand for caging-based grasping of free-flying object,” in *System Integration (SII), 2013 IEEE/SICE International Symposium on*. IEEE, 2013, pp. 436–442.
- [10] I. W. Park, T. Smith, S. W. Wong, P. Piacenza, and M. Ciocarlie, “Developing a 3-DOF compliant perching arm for a free-flying robot on the International Space Station,” in *Proc. IEEE Conf. on Robotics and Automation*, 2015.
- [11] G. J. Monkman, S. Hesse, R. Steinmann, and H. Schunk, *Robot grippers*. John Wiley & Sons, 2007.
- [12] Y. Mengüç, S. Y. Yang, S. Kim, J. A. Rogers, and M. Sitti, “Gecko-inspired controllable adhesive structures applied to micromanipulation,” *Advanced Functional Materials*, vol. 22, no. 6, pp. 1246–1254, 2012.
- [13] S. Kim, J. Wu, A. Carlson, S. H. Jin, A. Kovalsky, P. Glass, Z. Liu, N. Ahmed, S. L. Elgan, W. Chen, P. M. Ferreira, M. Sitti, Y. Huang, and J. A. Rogers, “Microstructured elastomeric surfaces with reversible adhesion and examples of their use in deterministic assembly by transfer printing,” *Proc. of the Natl. Academy of Sciences*, vol. 107, no. 40, pp. 17 095–17 100, 2010.
- [14] A. Parness, T. Hilgendorf, P. Daniel, M. Frost, V. White, and B. Kennedy, “Controllable on-off adhesion for earth orbit grappling applications,” in *Aerospace Conference, 2013 IEEE*. IEEE, 2013, pp. 1–11.
- [15] E. W. Hawkes, D. L. Christensen, A. K. Han, H. Jiang, and M. R. Cutkosky, “Grasping without squeezing: Shear adhesion gripper with fibrillar thin film,” in *Proc. IEEE Conf. on Robotics and Automation*, 2015, pp. 26–30.
- [16] H. Jiang, E. W. Hawkes, V. Arutyunov, J. Tims, C. Fuller, J. P. King, C. Seubert, H. L. Chang, A. Parness, and M. R. Cutkosky, “Scaling controllable adhesives to grapple floating objects in space,” in *Proc. IEEE Conf. on Robotics and Automation*, 2015.
- [17] M. Henrey, J. Tellez, K. Wormnes, L. Pambagian, and C. Menon, “Sticking in space: manufacturing dry adhesives and testing their performance in space environments,” in *12th Symp. on Adv. Space Technologies in Robotics and Automation*, 2013, pp. 15–17.
- [18] A. L. Ruina and R. Pratap, *Introduction to statics and dynamics*. Preprint for Oxford University Press, 2008.
- [19] E. W. Hawkes, H. Jiang, and M. R. Cutkosky, “Three-dimensional dynamic surface grasping with dry adhesion,” *International Journal of Robotics Research*, 2015.